

## Transverse Flow Effects In Dilepton Emission

K. Kajantie

August 1986

Collider Accelerator Department  
**Brookhaven National Laboratory**

**U.S. Department of Energy**

USDOE Office of Science (SC)

Notice: This technical note has been authored by employees of Brookhaven Science Associates, LLC under Contract No. DE-AC02-76CH00016 with the U.S. Department of Energy. The publisher by accepting the technical note for publication acknowledges that the United States Government retains a non-exclusive, paid-up, irrevocable, world-wide license to publish or reproduce the published form of this technical note, or allow others to do so, for United States Government purposes.

## **DISCLAIMER**

This report was prepared as an account of work sponsored by an agency of the United States Government. Neither the United States Government nor any agency thereof, nor any of their employees, nor any of their contractors, subcontractors, or their employees, makes any warranty, express or implied, or assumes any legal liability or responsibility for the accuracy, completeness, or any third party's use or the results of such use of any information, apparatus, product, or process disclosed, or represents that its use would not infringe privately owned rights. Reference herein to any specific commercial product, process, or service by trade name, trademark, manufacturer, or otherwise, does not necessarily constitute or imply its endorsement, recommendation, or favoring by the United States Government or any agency thereof or its contractors or subcontractors. The views and opinions of authors expressed herein do not necessarily state or reflect those of the United States Government or any agency thereof.

RHIC-PH-12

Transverse Flow Effects in Dilepton Emission

K. Kajantie, M. Kataja, L. McLerran, P.V. Ruuskanen

Brookhaven National Laboratory

August 1986

UNIVERSITY OF HELSINKI  
RESEARCH INSTITUTE FOR THEORETICAL PHYSICS  
SILTAVUORENPENGER 20 C . SF-00170 HELSINKI · FINLAND  
PREPRINT SERIES IN THEORETICAL PHYSICS  
NO: HU-TFT-86-6  
Jan. 24, 1986

TRANSVERSE FLOW EFFECTS IN  
DILEPTON EMISSION

K. Kajantie<sup>1)</sup>, M. Kataja<sup>2)</sup>, L. McLerran<sup>3)</sup> and P.V. Ruuskanen<sup>2)</sup>

Research Institute for Theoretical Physics, University of  
Helsinki, Helsinki, Finland

1) Academy of Finland and Department of Theoretical Physics,  
Siltavuorenpenger 20 C, SF-00170 Helsinki, Finland

2) Department of Physics, Seminaarinkatu 15, SF-40100 Jyväskylä,  
Finland

3) Fermilab., P.O. Box 500, Batavia, IL 60510, USA

ISBN 951-45-3888-9  
ISSN 0356-6331

Abstract

Dilepton emission from expanding QCD matter formed in ultra-relativistic nuclear collisions is computed. The energy density and the velocity field of the expanding matter are computed numerically with a 1+3 dimensional numerical code which assumes cylindrical invariance in the transverse and boost invariance in the longitudinal direction. Effects of transverse flow are studied and shown to be important in the region of pair mass  $M \lesssim 1.2$  GeV. The existence of transverse flow results in the persistent appearance of the  $\rho$  peak in the  $M$  distribution at fixed transverse mass  $M_T$  for large  $M_T$ . The initial temperature  $T_i$  and the thermalization time  $\tau_i$  of the hydrodynamical flow are related to the associated pion multiplicity  $dN/dy$  and the dilepton emission rate at  $M > 1.5$  GeV.

## 1. INTRODUCTION

A large amount of work has been devoted to studying possible signals for the production of QCD matter in its different phases as it might be formed in ultrarelativistic nucleus-nucleus collisions [1]. The physics which can be studied in such collisions includes the determination of state of hadronic matter, as well as properties of exotic new forms of matter such as quark-gluon plasma.

Because of the complexity of the problem, one has been forced to simplify the space-time history of the expanding matter. At best [2] one has coupled the dilution due to longitudinal boost invariant expansion [3] with transverse expansion using a one-phase equation of state.

The purpose of this paper is to consider the dilepton signal [4-9] by numerically computing [10-12] the matter flow assuming boost invariant longitudinal flow and cylindrical symmetry for the flow in the transverse direction and, secondly, assuming an equation of state containing a first order phase transition. The principal extension of the treatment of [2] of the transverse expansion is that we use an equation of state which allows one to continue past the quark-gluon plasma phase, through a phase transition and finally through a hadronic gas phase. This treatment involves using a hydrodynamic code which properly treats shock discontinuities and is discussed in [10]. In this paper we shall exclusively consider central collisions of heavy nuclei such as uranium.

What happens in the central region (at rest in the center of mass) of a central (zero impact parameter) U+U collision is essen-

tially as follows. Very early in the collision (at times less than  $1/M$ ) a single hard quark-antiquark collision may produce a massive dilepton pair through the Drell-Yan process. After this, collisions between the partons start thermalising the system. Dileptons may also be emitted during this pre-equilibrium stage [13-16]. During the pre-equilibrium stage the total comoving entropy  $S(\eta)$  of the system increases rapidly. From some proper time  $\tau_i$  and temperature  $T_i$  on,  $S$  is essentially constant and the system is regarded as thermalised. We shall in the following, unless otherwise stated, consider only the case when  $T_i$  is so large that the system initially is in the quark plasma phase. It may happen that this is not the case for an average experimental event.

Due to quantum fluctuations the value of  $S(\eta)$  may vary from event to event, but its value may be experimentally measured by measuring the associated pion multiplicity  $dN/dy$  and using the relationship [9]

$$S(\eta) = c \frac{dN}{dy}(\eta=y) = \pi R_A^2 4a T_i^3 \tau_i, \quad (1.1)$$

where  $c = 3.6$  and  $a = 4.6$  (for 2.5 flavours). Note that this only gives the combination  $T_i^3 \tau_i$ . The value of  $\tau_i$  is, however, not so well determined for a variety of reasons such as fluctuations in the initial conditions. In view of these uncertainties, we will consider  $\tau_i$  in the range of 0.1 to 1.5 fm. From the point of view of the hydrodynamic flow, this variation in the value of  $\tau_i$  is not important: increasing  $\tau_i$  from 0.1 fm to 1.5 fm gives, apart from small initial condition ( $v_r = 0$ ) effects, exactly the same flow, if  $T_i$  is simultaneously decreased by a factor  $(1.5/0.1)^{\frac{1}{3}}$  (Section 2). The change from the point of view of signals

is, however, significant, because the high temperature period between 0.1 and 1.5 fm in the history of the system would be excluded (Section 3).

Assume  $T_i$  is so large that the system initially is in the quark plasma phase. The system then will expand through quark, mixed and hadron phases [10-11]. We also assume that the nucleation of the first order transition is fast and do not discuss scenarios with phase separation [17] or deep supercooling [18]. What one finds (Section 2) is that the behaviour of the quark phase is little affected by the transverse flow. The longitudinal cooling is so fast that it cools the system out of the quark plasma phase before the transverse rarefaction wave reaches the center, i.e. before  $\tau = R_A/c_S \approx 12$  fm. Only for very large  $S_i$  does the quark phase experience transverse motion. However, one finds that when the system is in the mixed or even more so in the hadron phase, it is in very rapid transverse motion. For instance, in the numerical examples of Section 2 the temperature  $T = 50$  MeV (this is the lowest temperature we consider for the hadron gas) is reached at a proper time  $\tau = 35-65$  fm and the system is then essentially a disk of radius 15-50 fm in which the radial velocity varies from 0 at center to almost 1 at the sides.

How is this flow pattern experimentally diagnosed by dilepton emission? One finds (Section 3) that small  $M$  ( $M \lesssim 1.2$  GeV) pairs are dominantly emitted while the system is in the mixed and hadron phases. As the system then is in rapid transverse motion, the system imparts the pairs in this mass range a large transverse momentum. We find that the  $\rho$  peak will persist until largest transverse masses  $M_T$  for all reasonable values of the initial

temperature, formation time, and hadron multiplicity. Since the neglect of the transverse motion predicts the disappearance of the  $\rho$  peak [19], the observation of the  $\rho$  peak will permit one to experimentally identify the transverse flow. A different method of observing the flow is by comparing transverse momentum distributions of pions to those in pp at equivalent energy [10].

Similarly, the large  $M$  ( $M \gtrsim 2$  GeV) pairs are dominantly emitted while the system is in the quark phase. As this is the initial stage, one can now attempt to experimentally measure the values of  $T_i$  and  $\tau_i$  separately. First, a fixed value of  $T_i^3 \tau_i$  is chosen by considering only events with some fixed  $dN/dy$  of pions. Secondly, for these events one measures the rate  $dN/dMdy$  for pairs in the mass range  $2 < M < 3$ , say. The value of this rate depends on  $\tau_i$  separately and thus one can measure  $T_i$  and  $\tau_i$  separately. Note that this value of  $\tau_i$  (and the associated  $T_i$ ) is the average value of  $\tau_i$  for the events with the given  $dN/dy$ ; it is not the  $\tau_i$  for each event separately. The average value of  $\tau_i$  also contains an averaging over the transverse coordinates.

With dilepton measurements one has thus a fairly detailed handle on all the stages of the collision history from the earliest to the latest times. The required multiplicities are so large that the experiments are clearly very demanding. On the other hand, if either these large multiplicities are never produced in the collisions or if one is unable to experimentally observe them, one may never see evidence of these very interesting collective phenomena on the nuclear scale.

## 2. THE FLOW

The general features of a hydrodynamic flow through a quark plasma (Q), mixed (M) and hadron (H) phase under an assumed first order equation of state, have been discussed in several places (see, for instance, [10-11]) and we do not go into details here. Just to fix our notation, we note that our equation of state is, for the quark plasma and hadron phases, given by

$$\begin{aligned} P_q(T) &= g_q \frac{\pi^2}{90} T^4 - B, \\ P_h(T) &= g_h \frac{\pi^2}{90} T^4, \end{aligned} \quad (2.1)$$

where

$$\begin{aligned} g_q &= 2 \cdot 8 + 2 \cdot 5 + 2 \cdot 2 \cdot 3 \cdot \frac{7}{8} = 42.25, \\ g_h &= 3 \end{aligned} \quad (2.2)$$

(we use  $N_F = 2.5$  to simulate the effect of the strange quark mass). Many quantities depend only on the ratio

$$r = \frac{g_q}{g_h} \approx 14. \quad (2.3)$$

The bag constant  $B$  and the transition temperature  $T_c$  are related by

$$B = (g_q - g_h) \frac{\pi^2}{90} T_c^4 \quad (2.4)$$

and the values of the energy density in the quark and hadron phases at  $T_c$  are

$$\begin{aligned} \epsilon_q(T_c) &\equiv \epsilon_Q = \epsilon_H + 4B, \\ \epsilon_h(T_c) &\equiv \epsilon_H = \frac{3B}{r-1}. \end{aligned} \quad (2.5)$$

We shall mostly use the value  $T_c = 200$  MeV for the transition temperature and  $T_f = 50$  MeV for the decoupling temperature. These correspond to (in units of  $\text{GeV}/\text{fm}^3$ )

$$\begin{aligned} \epsilon_Q &= 3.62, \\ \epsilon_H &= 0.21, \\ \epsilon_f &= 0.001. \end{aligned} \quad (2.6)$$

In the hydrodynamic flow with no transverse motion the times between the different phases are given by

$$\begin{aligned} \tau_Q &= \left( \frac{T_i}{T_c} \right)^3 \tau_i, \\ \tau_H &= r \tau_Q, \\ \tau_f &= \left( \frac{T_c}{T_f} \right)^3 \tau_H. \end{aligned} \quad (2.7)$$

Note here that a proper treatment of decoupling from the hadron phase would require the use of kinetic theory. The use of hydrodynamics down to  $T_f = 50$  MeV in the dilepton emission calculations below is to be understood as an estimate of the upper limit of the contribution from the hadron phase. A conservative lower limit is obtained by including only the mixed phase (i.e., increasing  $T_f$  to  $T_c$ ) and the results from this estimate are in qualitative accord with the results obtained with  $T_f = 50$  MeV.

The hydrodynamic flows corresponding to the parameters in Table 1 were computed using the methods of [10] and some of the results are exhibited in Figs. 2.1-5. One can observe the following (the sizes and lifetimes given below refer, for definiteness,

to a decoupling temperature  $T_f = 50$  MeV; sizes corresponding to other values of  $T_f$  can be read from the figures):

(1) At  $T_i = 250$  MeV,  $\tau_i = 1$  fm, the quark phase lasts only very briefly, from 1 to 2 fm, and its transverse motion is totally negligible. Even the mixed phase is hardly at all affected by transverse motion, while the hadron phase moves in the transverse direction. The system lives for about 35 fm and its largest transverse extent is 17 fm.

(2) At  $T_i = 500$  MeV,  $\tau_i = 0.5$  fm, the value of  $\tau_Q (= 7.8$  fm) is already so close to the transverse time-scale  $R_A/c_s \approx 12$  fm) that there appears a moderate buildup of transverse expansion at the sides of the quark phase. As a result large parts of the mixed phase and the entire hadron phase flow transversally. This reduces significantly the growth of the life-time of the system (relative to  $v_T = 0$ ), which now is 50 fm, the largest transverse extent being 30 fm.

(3) The flows with  $T_i = 350$  MeV,  $\tau_i = 1.5$  fm and  $T_i = 833$  MeV,  $\tau_i = 0.11$  fm have the same  $T_i^3 \tau_i$ , i.e., the same  $dN/dy$ . They are thus expected to be essentially the same flows, just started at different times and, correspondingly, different temperatures. This is verified by the numerical computation (results not shown). Actually small differences, caused by initial transverse velocity effects, appear: if we vary  $\tau_i$  between 1.4, 0.5 and 0.11 fm, the transverse velocity field clearly cannot be assumed to vanish at all these times. The differences thus also give a feeling of the effects of changing the initial radial velocity.

(4) At  $T_i = 833$  MeV and  $\tau_i = 0.33$  fm  $\tau_Q = 24$  fm is much larger than the transverse time scale and also the quark phase is

set in transverse motion. Thus also its life-time is reduced from the value 24 fm, valid for no transverse motion, to about 12 fm. Due to the rapid transverse motion the life-time of the mixed phase is reduced even relative to the previous  $dN/dy = 26$  case, but ultimately the system lives long as a very dilute pion gas (more properly treated by kinetic theory) so that its total life-time is 65 fm and its largest extent about 50 fm.

Note that physically this example is rather extreme. The initial energy density implied in this circumstance corresponds to all of the kinetic energy of the two nuclei being deposited in a rapidity interval of one unit when the collision energy is 100+100 GeV.

(5) If  $T_C$  is decreased from 200 MeV to 160 MeV, everything else remaining unchanged, the qualitatively essential change is the increase of  $\tau_Q$  by a factor 2.0. This implies that already the quark phase is set in rapid transverse motion, which further propagates to the mixed and hadron phases. The expected net result is an increase in the space-time volume of the quark phase, a decrease in that of the mixed and hadron phases, and an increase in the overall transverse motion. The expectations are born out by the numerical computation (results in Fig. 2.4).

(6) All the above flows assume that  $T_i$  is independent of  $r$ . The expected  $r$  dependence is correlated with the  $A$  dependence of  $dN/dy$ : if

$$\frac{dN}{dy} \propto A^{\frac{2}{3}(U+P)},$$

then

$$S_i(r) \tau_i \propto \left(1 - \frac{r^2}{R_A^2}\right)^P$$



We expect  $p$  to be about  $1/2$ ,  $p = 1$  being a rather extreme value. The flow corresponding to this extreme  $r$  dependence,

$$T_i(r) = T_{i0} \left(1 - \frac{r^2}{R_A^2}\right)^{\frac{1}{2}}, \quad (2.8)$$

with  $\tau_i = 0.5$  and  $T_{i0} = 630$  MeV (so that the total entropy of the flow is normalised to the same value  $dN/Ady = 26$  as for the flow with  $T_i = 500$  MeV,  $\tau_i = 0.5$  fm) is given in Fig. 2.5. As expected, the transverse flow is now more rapid. Even the mixed phase now flows transversally and its life-time near  $r = 0$  is considerably reduced, less so at larger  $r$ . However, now the system lives longer in the hadron phase so that the total life-time at  $r = 0$  is about the same as with constant  $T_i$ .

The huge life-times of the mixed and hadron phases (Table 1) in the approximation  $v_r = 0$  are thus considerably reduced. Still, this reduction in the time direction is partially compensated by the expansion of the system in the transverse direction.

### 3. EMISSION OF DILEPTONS

The calculation of dilepton emission rate per collision proceeds straightforwardly by convoluting the rest frame emission rates from the quark plasma and the hadron phases with the flows computed above. In the mixed phase, the system emits both from the quark and hadron phases, the relative amount of these being given by entropy conservation.

The emission rate from the quark phase is well known to be

$$\frac{dN}{d^4x dM^2 d^3p/E} = \frac{\alpha^2}{8\pi^4} \sum e_i^2 e^{-E/T}. \quad (3.1)$$

The calculation of the emission rate from the hadron is much more complicated [6]. Since we model the hadron phase by a pion gas, we only include the process  $\pi^+\pi^- \rightarrow \ell^+\ell^-$  and include only the  $\rho$  pole in the form factor:

$$F^2(M) = \frac{m_\rho^4}{(m_\rho^2 - M^2)^2 + m_\rho^2 \Gamma_\rho^2}, \quad (3.2)$$

with  $m_\rho = 0.77$  and  $\Gamma_\rho = 0.155$  GeV. With this form factor, the emission rate is

$$\frac{dN}{d^4x dM^2 d^3p/E} = \frac{\alpha^2}{8\pi^4} \left(1 + \frac{2m_\pi^2}{M^2}\right) \left(1 - \frac{4m_\pi^2}{M^2}\right) \frac{1}{12} F^2(M) e^{-E/T}. \quad (3.3)$$

This could be improved by including more resonances in the form factor or, even better, by using  $e^+e^-$  data for pion production. Also, one might want to include a temperature dependent mass and width [20-21] for the  $\rho$ , to obtain a method for experimentally testing these  $T$  dependences. If the  $\rho$  significantly alters its mass in the pion phase, this shift might indeed appear in the experimentally observed dilepton spectrum. The degree of such a shift near the deconfinement temperature in the hadron phase is unknown. However, the main approximation is probably the neglect of bremsstrahlung production of dileptons:  $\pi^+\pi^- \rightarrow \pi^+\pi^- \gamma^*$ . This will certainly dominate in the region  $M < 2m_\pi$ . It can be calculated, but the calculation is technically rather complicated. We believe that the simple  $\rho$  pole approximation used here is quite adequate for pair masses near the  $\rho$  mass and above.

We are also neglecting the sharp resonances  $\phi$  [22] and  $\psi$  [23]. A calculation of their production rate with the above realistic numerical flows would be another interesting problem. Since the  $\psi$  mass is so large, it is emitted very early in the collision from the quark plasma phase and we actually expect the no-transverse-flow approximation of ref. [23] to be good.

The convolution over the flow is now of the form

$$\begin{aligned} \frac{dN}{dM^2 dy d^2 p_T} &= \int d^4 x e^{-u \cdot p / T} \\ &= \int \tau dr d\eta r dr d\varphi \exp \left\{ -\frac{\gamma_r}{T} \left[ M_T \cosh(\eta - y) - v_r p_T \cos \varphi \right] \right\} \\ &= 4\pi \int \tau dr r dr K_0 \left( \frac{\gamma_r M_T}{T} \right) I_0 \left( \frac{\gamma_r v_r p_T}{T} \right), \end{aligned} \quad (3.4)$$

where we have used

$$\begin{aligned} \tau &= (t^2 - z^2)^{\frac{1}{2}}, \\ \eta &= \frac{1}{2} \log \frac{t+z}{t-z}, \\ u^\mu &= \gamma_r \left( \frac{t}{\tau}, v_r \cos \varphi, v_r \sin \varphi, \frac{z}{\tau} \right), \\ p^\mu &= (E, p_T, 0, p_L) \\ M_T &= (M^2 + p_T^2)^{\frac{1}{2}}, \quad E = M_T \cosh y, \end{aligned}$$

and  $K_0$  and  $I_0$  are modified Bessel functions. The transverse velocity  $v_r$  ( $\gamma_r = 1/(1-v_r^2)^{\frac{1}{2}}$ ) and the temperature  $T$  are given as functions of  $\tau$  and  $r$  by the numerical calculation of the flow.

Noting that the relative volumes of the quark plasma and hadron phases within the mixed phase are given by

$$\frac{V_Q}{V} = \frac{\epsilon - \epsilon_H}{\epsilon_Q - \epsilon_H}, \quad \frac{V_H}{V} = \frac{\epsilon_Q - \epsilon}{\epsilon_Q - \epsilon_H},$$

we can write the dilepton rate in the final form

$$\frac{dN}{dM^2 dy d^2 p_T} = \frac{\alpha^2}{2\pi^3} \int \tau dr r dr I_0 \left( \frac{\gamma_r v_r p_T}{T} \right) K_0 \left( \frac{\gamma_r M_T}{T} \right). \quad (3.5)$$

$$\cdot \left\{ \sum e_q^2 \theta(Q) + \left[ \frac{\epsilon - \epsilon_H}{\epsilon_Q - \epsilon_H} \sum e_q^2 + \frac{\epsilon_Q - \epsilon}{\epsilon_Q - \epsilon_H} G(M^2) \right] \theta(M) + G(M^2) \theta(H) \right\},$$

where the  $\theta$  functions test whether  $\epsilon > \epsilon_Q$  ( $\theta(Q)$ ),  $\epsilon_H < \epsilon < \epsilon_Q$  ( $\theta(M)$ ) or  $\epsilon_F < \epsilon < \epsilon_H$  ( $\theta(H)$ ) and (we take  $m_s = 0$ )

$$G(M^2) = \frac{1}{12} F^2(M) \left( 1 - \frac{4m_\pi^2}{M^2} \right).$$

Further, the result (3.5) can be integrated analytically over the  $p_T$  of the emitted dilepton with the result

$$\frac{dN}{dM^2 dy} = \frac{\alpha^2}{\pi^2} \int \tau dr r dr M T K_1 \left( \frac{M}{T} \right) \{ \dots \}, \quad (3.6)$$

where the curly bracket is the same as in (3.5). Surprisingly,  $v_r$  does not at all appear in Eq. (3.6). The result looks very simple, but  $T$  (and the  $\epsilon$  in the curly bracket) are only given by the numerical hydro as functions of  $\tau$  and  $r$ .

If the radial flow is neglected ( $v_r = 0$ ), the above results simplify to the form

$$\frac{dN}{dM^2 dy d^2 p_T} = \frac{\alpha^2}{4\pi^4} \pi R_A^2 (T_i^3 \tau_i)^2 \frac{3}{M_T^6} \left\{ \int_{M_T/T_i}^{M_T/T_c} dy y^5 K_0(y) \sum e_f^2 + \right. \\ \left. + \frac{r-1}{18} [\sum e_f^2 + r G(M^2)] \left(\frac{M_T}{T_c}\right)^6 K_0\left(\frac{M_T}{T_c}\right) + r^2 \int_{M_T/T_c}^{M_T/T_f} dy y^5 K_0(y) G(M^2) \right\} \quad (3.7)$$

and

$$\frac{dN}{dM^2 dy} = \frac{\alpha^2}{4\pi^4} \pi R_A^2 (T_i^3 \tau_i)^2 \frac{6\pi}{M^4} \left\{ \int_{M/T_i}^{M/T_c} dy y^4 K_1(y) \sum e_f^2 + \right. \\ \left. + \frac{r-1}{18} [\sum e_f^2 + r G(M^2)] \left(\frac{M}{T_c}\right)^5 K_1\left(\frac{M}{T_c}\right) + r^2 \int_{M/T_c}^{M/T_f} dy y^4 K_1(y) G(M^2) \right\} \quad (3.8)$$

Within the domain of validity of the approximations, one could replace the Bessel functions by  $K_m(y) = (\pi/2y)^{\frac{1}{2}} \exp(-y)$ .

#### 4. NUMERICAL RESULTS

The formulas given for the dilepton rate in Section 3 are easily integrated over the flows in Section 2. Results are given in Figs. 4.1-8. Note that we give all numbers as rates per a collision at zero impact parameter  $b$ . The experiments will anyway attempt to trigger for central collisions and averages over  $b$  are not needed. However, when comparing with a Drell-Yan rate (which is averaged over  $b$ ), the averaging has to be taken into account. The rates can be turned to cross sections by multiplying with  $\sigma = \pi (R_A + R_B)^2$  (and dividing by  $(1 + R_A/R_B)^2$ , if

averaging over  $b$  is required).

Fig. 4.1 gives the wholly differential rate  $dN/dM^2 dy d^2 p_T$  for the flow with  $T_i = 500$  MeV,  $\tau_i = 0.5$  fm, corresponding to  $dN/dy = 26$ . For comparison, the same quantity is given in Fig. 4.2 calculated if only longitudinal cooling with no transverse flow is included, in Fig. 4.3 for a flow which has the same comoving entropy but which starts later, at  $\tau_i = 1.5$  fm corresponding to  $T_i = 350$  MeV and in Fig. 4.4 for a flow starting at  $\tau_i = 0.5$  with the same comoving entropy but with an initially  $r$  dependent temperature distribution (Eq. (2.8)).

Consider first the quark plasma contribution, which has, in detail, been studied in refs. [8-9]. This is "the new phase of matter" one expects to diagnose with these dilepton measurements. It is formed very early in the process and thus, as is explicitly shown by the figures in Section 2 and a comparison of Figs. 4.1 and 4.2, the transverse flow has little effect on it. If one goes to details, one observes that the transverse flow reduces somewhat the rate and the reduction is largest at small  $M_T$ . This is natural, since small  $M_T$  pairs are dominantly produced late in the quark plasma phase, so that the transverse flow has had time to penetrate towards the center and further reduce the temperature.

Another consequence of the insensitivity of the quark matter contribution to the transverse flow is that the rate from it is essentially independent of the pair mass  $M$  when plotted against  $M_T$ . For the  $v_r = 0$  case this observation was made already in ref. [8].

Another relevant remark can be made by considering two different flows having the same total entropy, i.e., the value

of  $T_i^3 \tau_i$ . If we change the value of  $\tau_i$  from 0.5 fm to 1.5 fm (as in Figs. 4.1 and 4.3), the flow after 1.5 fm is unchanged, if the initial condition at 1.5 fm is taken to be the initial condition at 0.5 fm hydrodynamically evolved to 1.5 fm. In the calculations of Section 2 actually  $v_r = 0$  was used as the initial condition at both times. This causes a small change in the later flows. Apart from this small change, the only change in the dilepton rate is then that, when increasing  $\tau_i$  from 0.5 fm to 1.5 fm, we lose the contribution from this time interval. As the matter then is in very hot quark plasma phase (between  $T = 350$  and  $500$  MeV), the loss is essentially in the production of large  $M_T$  pairs. In the case of Figs. 4.1 and 4.3 this loss is an order of magnitude or more at  $M_T > 3.5$  GeV. We again emphasize that this effect is an early-time large- $M_T$  effect and thus independent of transverse flow.

Ideally, one could use the sensitivity of the large  $M_T$  dilepton rate to very early times to experimentally determine the initial thermalization time  $\tau_i$  and temperature  $T_i$  separately as follows. First separate the dilepton events according to the value of the associated pion multiplicity  $dN/dy$ . This (given  $R_A$ ), fixes the value of the product  $T_i^3 \tau_i$  according to Eq. (1.1). Considering now this fixed value of  $dN/dy$  one measures the rate of dilepton production at large  $M_T$ . Its value depends on  $T_i$  and  $\tau_i$  separately and, when measured, can thus be used to give a numerical value for  $\tau_i$  and  $T_i$  separately. This is not a value of  $\tau_i$  for each event separately (as is the product  $T_i^3 \tau_i$ ) but an average  $\tau_i$  for all the events having a fixed value of  $T_i^3 \tau_i$ . Since the initial value of  $T_i$  may and will depend on  $r$  and will also stochastically fluctuate across the nuclear disc, the measured value of  $\tau_i$  will also contain and average across the transverse coordinate.

Note also that  $M_T$  should neither be so large that one is in the single-collision Drell-Yan region nor even in the intermediate pre-equilibrium region. We shall give an estimate for this when discussing  $dN/dMdy$  below.

Consider then the mixed phase and hadron phase contributions. A comparison between Figs. 4.1 and 4.2 shows that the result for correct transverse flow is significantly different from that obtained by taking  $v_r = 0$  (Eqs. (3.7-8)): the rate at small  $M_T$  is reduced by orders of magnitude and at large  $M_T$  increased by orders of magnitude. This is a direct effect of the transverse flow. Pairs with  $M < 1$  GeV are dominantly emitted at late times from relatively cool matter, which is moving transversally with a large velocity (see the Figs. in Section 2). This imparts a large  $p_T$  to the particles and makes the  $M_T$  distribution much flatter than for  $v_r = 0$ . For  $v_r = 0$  the  $M_T$  distribution of pairs from the mixed phase goes (Eq. (3.7)) like

$$K_0\left(\frac{M_T}{T_c}\right) \sim M_T^{-\frac{1}{2}} e^{-M_T/T_c}$$

(this also holds for H if  $M_T > 5T_c$ ). For true flow this is found to be much flatter but not quite as flat as  $\exp(-M_T/T_i)$ .

The transverse flow effect is particularly clear if one chooses a mass which maximizes the M and H contributions relative to Q: the region near  $M = m_\rho$ . From Figs. 4.1 and 4.3 it is clear that M and H will dominate over Q at all values of  $M_T$ . In detail the persistence of the  $\rho$  peak is shown in Fig. 4.5. Its relative importance thus even increases with increasing  $M_T$ . This situation is quite different from that at  $v_r = 0$ . As is seen from Fig. 4.2, the  $\rho$  peak there will vanish under the mass-independent quark plasma contribution for  $M_T > 3$  GeV [19]. The observation of the

$\rho$  peak at large  $M_T$  would be direct evidence for a collective flow of a hadronic system. It is hard to see how this effect could be reproduced by the various models for particle production in nucleus-nucleus collisions, which make no reference to collective behaviour. This clearly is an issue deserving further study.

As seen from Fig. 4.4, the persistence of the  $\rho$  peak is also stable against introducing  $r$  dependence in the initial temperature, although the flows in the mixed phase seem considerably different (compare Figs. 2.2 and 2.5). The rapid evolution of the system in the mixed phase in Fig. 2.5 means that energy is not wasted in longitudinal expansion. It goes into transverse expansion and maintains the large emission rate into large  $M_T$  near  $M = m_\rho$ .

Consider then the results for the  $p_T$ -integrated rate  $dN/dMdy$  (Eq. (3.6)), shown in Figs. 4.6-8. At this point it is also convenient to compare the result with the Drell-Yan background. A rough estimate for this at  $M \ll \sqrt{s}$  is

$$\frac{dN_{A+A}^{DY}}{dM dy} = 4 \cdot \frac{A^{\frac{4}{3}} \cdot 3.8 \cdot 10^{-8}}{M^3} \left[ \frac{4\pi R_A^2}{\sigma_{in}} \right] \left[ \frac{S^A(0) + \text{valence-sea effects}}{0.95A} \right] \quad (4.1)$$

which is directly obtained from the standard Drell-Yan formula (no K factor) and in which we expect the square brackets to be of order one. The factor 4 in front corrects the formula for central collisions and  $M$  is expressed in GeV units to give the result in  $1/\text{GeV}$ . If  $T_i$  is clearly above  $T_c$ , the Drell-Yan background is clearly below thermal emission for the range of masses shown ( $M < 3 \text{ GeV}$ ); for high dilepton masses the Drell-Yan rate

will, of course, ultimately win. For  $T_i = 250 \text{ MeV}$  (Fig. 4.8) there is so little of the quark plasma phase that the Drell-Yan mechanism-especially if supplemented by the so far uncalculated pre-equilibrium emission-gives a relatively large contribution.

The following comments can be made concerning Figs. 4.6-8. The three parts of Fig. 4.6 illustrate, as discussed above, how one gains more quark plasma contribution by starting the flow earlier. The gain is from high temperatures and goes, accordingly, to large dilepton masses. The quantitative observation of the high mass-tail in Fig. 4.6 is precisely "diagnosis of quark plasma". Fig. 4.7 illustrates what happens if  $T_c$  is decreased from 200 to 160 MeV. As discussed in Section 2, the quark phase then lasts longer at temperatures close to  $T_c$ . The small-mass part of  $Q$  is thus somewhat increased. The  $M$  and  $H$  contributions decrease above the  $\rho$  faster at  $T_c = 160 \text{ MeV}$ , roughly proportionally to  $\exp(-M/T_c)$ . However, at this large  $T_i$  it is not possible to observe this behaviour, since it is hidden below the large  $Q$  contribution. To measure the value of  $T_c$  one has to go to smaller values of  $T_i$  (Fig. 4.8). The  $Q$  term then is much smaller and the  $\exp(-M/T_c)$  behaviour is exposed. However, the Drell-Yan contribution is threateningly close.

We conclude this section by noting that the calculated  $dN/dMdy$  for produced dilepton pairs in the  $\rho$  mass region can be used to estimate the number of  $\pi\pi$  collisions which took place in the mixed and hadron phases. The pions namely dominantly interact via the  $\rho$  resonance (apart from  $\pi^0\pi^0$ ) and what we have calculated is how often this resonance, after a life-time of about 1 fm, decays to a dilepton pair. To estimate the total number of interactions we simply write

$$\text{Number of } \pi\pi \text{ collisions} = \frac{3\Gamma_g}{B(g \rightarrow e^+e^-)} \frac{dN}{dMdy}, \quad (4.2)$$

where the 3 accounts for  $\pi^+\pi^0$ ,  $\pi^+\pi^-$  and  $\pi^-\pi^0$ . For instance, for the  $T_1 = 500$  MeV,  $\tau_1 = 0.5$  fm case this gives about 3000 interactions in the mixed phase and 1500 in the hadron phase. Counting collisions per particle gives a further factor of two. In the mixed phase there are in addition pion-quark and pion-gluon interactions. There should not be too much difficulty maintaining thermal equilibration in the mixed phase. In the hadron phase, this is however enough for kinetic theory but marginally so for hydrodynamics. Note also that these final remarks are in agreement with the standard observation that essentially all the pions produced in hadronic collisions are produced via the  $\rho$ . This observation just counts the last interaction via a  $\rho$  as the produced particle, while we have been considering the pions produced in the previous interactions as elements of the hadronic fluid.

## 5. CONCLUSIONS

We have in this paper considered the effects of transverse collective flow of QCD matter as it might be formed in ultra-relativistic nucleus-nucleus collisions. This is clearly an important question; we cannot really talk about "matter", unless we can prove that the system behaves collectively. The question of the existence of collective flow has also been a central issue in connection of nuclear collisions in the 1 GeV range [24].

Under reasonable initial conditions, the quark plasma phase is formed, if at all, very early in the collision. It thus is little affected by transverse motion and its collective motion is essentially longitudinal. This, however, is next to impossible to separate from the longitudinal motion, which is anyway present in the produced particles. Instead, we have attempted to discuss how the parameters  $T_1$  and  $\tau_1$  of the flow could be determined.

The situation is quite different with the later stages of the process. If the system has started high up in the quark plasma phase, it is already in rapid transverse motion after having cooled down to the mixed phase. Whatever is emitted at this stage, will get a boost in the transverse direction from this motion. As the system is already rather cool, it will dominantly emit dileptons in the 1 GeV mass range and we have shown that this emission from matter in transverse motion may lead to the persistence of the  $\rho$  peak until very large  $M_T$ . The effect is further amplified by the emission from the very late and cool hadron phase, which should properly be treated with kinetic theory.

If the persistence of the  $\rho$  peak at large  $M_T$  is experimentally observed, one further has to prove that this cannot convincingly be reproduced by any of the mechanisms of particle production not containing collective motion. The discussion will perhaps parallel that around cascade vs. collective models in the 1 GeV range [25].

Concerning the experimental observation of the effects discussed here one should note that an average A+A event might have  $T_1 = T_C$  and starts expansion in the mixed phase. For the

effects to be fully developed, the expansion time has to be long and the system must start at high temperature in the quark plasma phase, the higher the better. One will thus be studying the tail of the multiplicity distribution and the length of this tail will determine how well these collective effects can be studied. The average and the width of the multiplicity distribution are crucial unknown parameters, on which even the first generation relativistic heavy ion experiments will give important information.

Acknowledgements: We have profited from discussions with P. Glässel, J. Kapusta and A. Mekjian.

#### REFERENCES

1. For a review of the present state of quark matter physics, see Proceedings of Quark Matter '84, ed. K. Kajantie, Springer Verlag, 1985 or Proceedings of the RHIC workshop, ed. by P. Hausteijn and C. Woody, BNL report 51921, 1985.
2. Gordon Baym, B. Friman, J.-P. Blaizot, M. Soyeur and W. Czyz, Nucl. Phys. A407, 541 (1983).
3. J.D. Bjorken, Phys. Rev. D27, 140 (1983).
4. E.L. Feinberg, Nuovo Cimento 34A, 39 (1976); E. Shuryak, Phys. Lett. 78B, 150 (1978), Yad. Fiz. 28, 796 (1978) [Sov. J. Nucl. Phys. 28, 1548 (1978)].
5. V. Cerny, P. Lichard and J. Pisut, Phys. Lett. 70B, 61 (1977); Phys. Rev. D16, 2822 (1977), Phys. Rev. D18, 2409 (1978), Phys. Rev. D24, 652 (1981).
6. G. Domokos and J. Goldman, Phys. Rev. D23, 203 (1981), G. Domokos, Phys. Rev. 28, 123 (1980).
7. K. Kajantie and H.I. Miettinen, Z. Phys. C9, 341 (1981); C14, 357 (1982).
8. L.D. McLerran and T. Toimela, Phys. Rev. D31, 545 (1985).
9. R. Hwa and K. Kajantie, Phys. Rev. D32, 1109 (1985).
10. E. von Gersdorff, M. Kataja, L. McLerran and P.V. Ruuskanen, Fermilab preprint 86/13-T, 1986.
11. B. Friman, K. Kajantie and P.V. Ruuskanen, Nucl. Phys. B266, 468 (1986).
12. A. Białas, W. Czyz and A. Kolawa, Acta Physica Polonica B15, 229 (1984); S. Pratt, Univ. of Minnesota preprint, June 1985.
13. A. Białas and J.-P. Blaizot, Phys. Rev. D32, 2954 (1985).
14. K. Kajantie and T. Matsui, Phys. Lett. 164B, 373 (1985).
15. M. Gyulassy and A. Iwazaki, Phys. Lett. 165B, 157 (1985).
16. A. Kerman, T. Matsui and B. Svetitsky, MIT preprint CTP 1299, 1985.
17. L. Van Hove, Z. Phys. C27, 135 (1985).

18. M. Gyulassy, K. Kajantie, H. Kurki-Suonio and L. McLerran, Nucl. Phys. B237, 477 (1984);  
N.K. Glendenning and T. Matsui, Phys. Lett. 141B, 419 (1984);  
B. Friman, Phys. Lett. 159B, 369 (1985).
19. P. Siemens and S.A. Chin, Phys. Rev. Lett. 55, 1266 (1985).
20. A.I. Bochkarev and M.E. Shaposnikov, Phys. Lett. 145B, 276 (1984)
21. R. Pisarski, Phys. Lett. 110B, 155 (1982).
22. A. Shor, Phys. Lett. 54, 1122 (1985).
23. J. Cleymans and C. Vanderzande, Phys. Lett. 147B, 186 (1984).
24. H.A. Gustafsson et al., Phys. Rev. Lett. 52, 1590 (1984).
25. J. Cugnon, in the first of refs. [1].

TABLE 1. Values of parameters used (in units of MeV or fm,  $A = 238$ ). Note the logic in the table: the primary quantity is the associated pion multiplicity  $dN/dy$ , which can be experimentally fixed and which fixes  $T_i^3 \tau_i$ . All the flows with the same  $dN/dy$  and  $T_c$  have the same one-dimensional ( $v_r = 0$ ) time-scales (Eq. (2.7)). Changing  $T_c$  changes the relative balance of Q and M but not the total one-dimensional duration. The true three-dimensional life-times are discussed in Section 2 (see (Figs. 2.1-5)).

$dN/dy$	$T_i$	$T_c$	$\tau_i$	$\tau_Q$	$\tau_H$	$\tau_f$
6.4	250	200	1.0	1.9	27	1800
26	350	200	1.5	7.8	110	7000
26	500	200	0.5	7.8	110	7000
26	833	200	0.11	7.8	110	7000
26	500	160	0.5	15	215	7000
78	833	200	0.33	24	340	21500



FIGURE CAPTIONS

- Fig. 2.1 Curves of (a) constant energy density (in units of  $\text{GeV}/\text{fm}^3$ ) and (b) constant radial velocity for  $T_i = 250$  MeV,  $\tau_i = 1$  fm and  $T_c = 200$  MeV. The velocity contours near the light cone in this and the following figures are an artifact of the numerical method and graphics and have no physical meaning.
- Fig. 2.2 As Fig. 2.1 but for  $T_i = 500$  MeV and  $\tau_i = 0.5$  fm. The curves for the cases having the same  $dN/dy$  in Table 1 are essentially the same apart from the starting time  $\tau_i$  of the flow.
- Fig. 2.3 As Fig. 2.1 but for  $T_i = 833$  MeV and  $\tau_i = 0.33$  fm.
- Fig. 2.4 As Fig. 2.2 but for  $T_c = 160$  MeV.
- Fig. 2.5 As Fig. 2.2 but for the radially varying initial temperature distribution in Fig. Eq. (2.8).
- Fig. 4.1 The quark phase (Q), mixed phase (M) and hadron phase (H) contributions to the differential dilepton production rate  $dN/dM^2 dy d^2 p_T$  plotted vs.  $M_T$  for  $M = 0.3, 0.8$  and  $1.5$  GeV for the flow with  $T_i = 500$  MeV and  $\tau_i = 0.5$  fm. Up to negligible corrections the Q contribution is independent of pair mass  $M$  when plotted vs.  $M_T$ .
- Fig. 4.2 As Fig. 4.1 but for zero radial flow: Q is independent of pair mass  $M$ .
- Fig. 4.3 As Fig. 4.1 but for the flow with  $T_i = 350$  MeV,  $\tau_i = 1.5$  fm. This flow has the same comoving entropy as the one in Fig. 4.1.
- Fig. 4.4 As Fig. 4.1 but now calculated for the flow in Fig. 2.5 with the radially varying initial temperature distribution in Eq. (2.8).
- Fig. 4.5 As Fig. 4.1 but now plotted vs.  $M$  for transverse masses  $M_T = 1, 2,$  and  $4$  GeV. The dashed lines show the separate contributions of the different phases at  $M_T = 4$ . Note the persistence and even strengthening of the  $\rho$  peak. The  $\rho$  peak persists even if the hadron phase contribution is neglected.
- Fig. 4.6 The quark phase (Q), the mixed phase (M), the hadron phase (H) contributions and the total differential dilepton production rate  $dN/dM dy$  plotted vs. pair mass  $M$  for the three flows (a)  $T_i = 350$  MeV,  $\tau_i = 1.5$  fm, (b)  $T_i = 500$  MeV,  $\tau_i = 0.5$  fm, (c)  $T_i = 833$  MeV,  $\tau_i = 0.11$  fm having the same associated pion multiplicity  $dN/dy = 26 \lambda$  (Table 1). Note how M and H are essentially unchanged while the large-M behaviour of Q increases when  $\tau_i$  is decreased and more of the hotter initial matter is included.
- Fig. 4.7 As Fig. 4.6 (b) but for  $T_c = 160$  MeV.
- Fig. 4.8 As Fig. 4.6 but for the flow with  $T_i = 250$  MeV,  $\tau_i = 1$  fm. The dashed line gives the single-scattering Drell-Yan contribution according to Eq. (4.1).

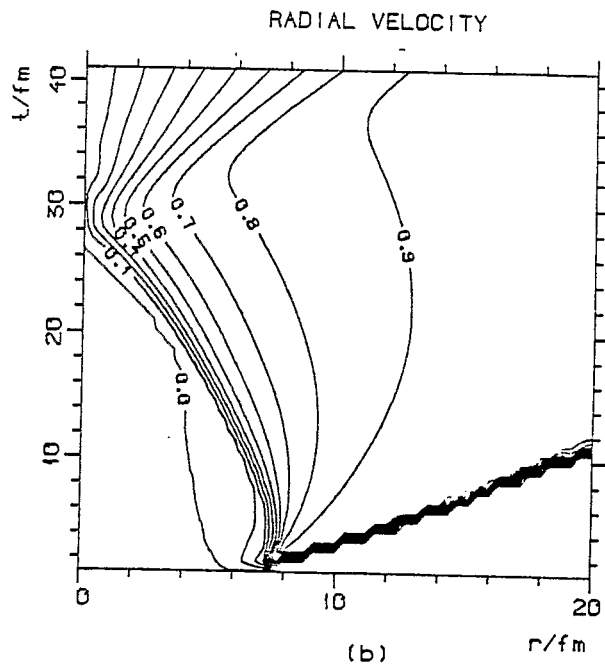
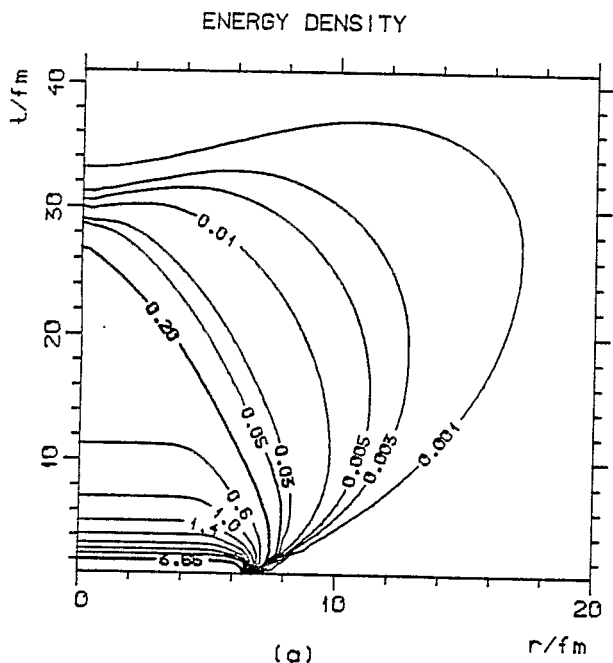


Fig. 2.1

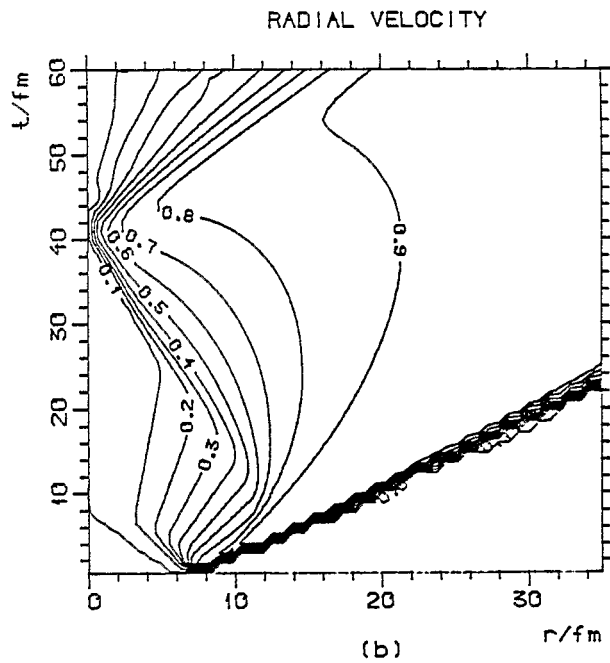
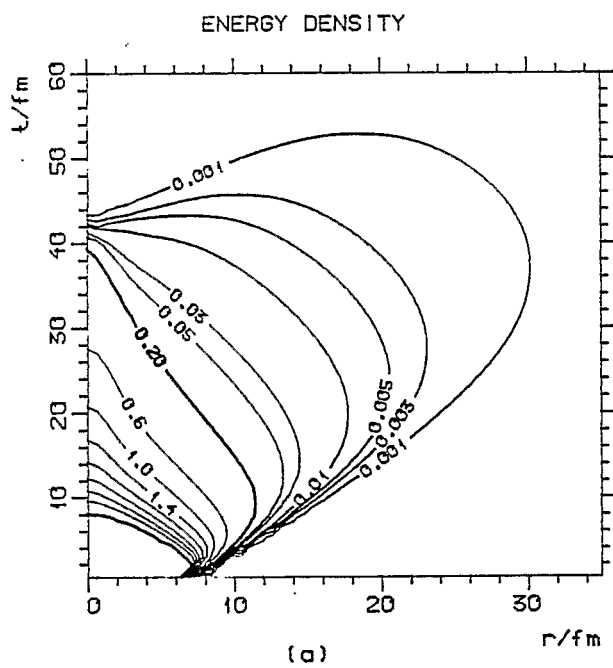


Fig. 2.2

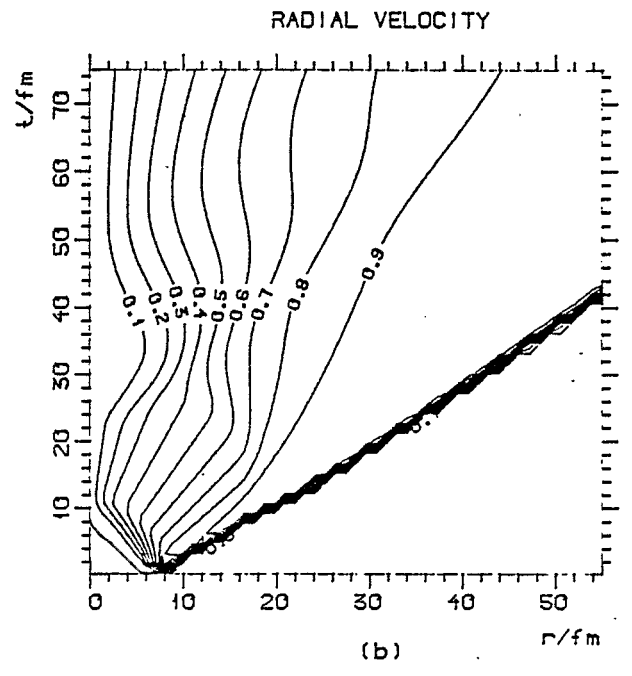
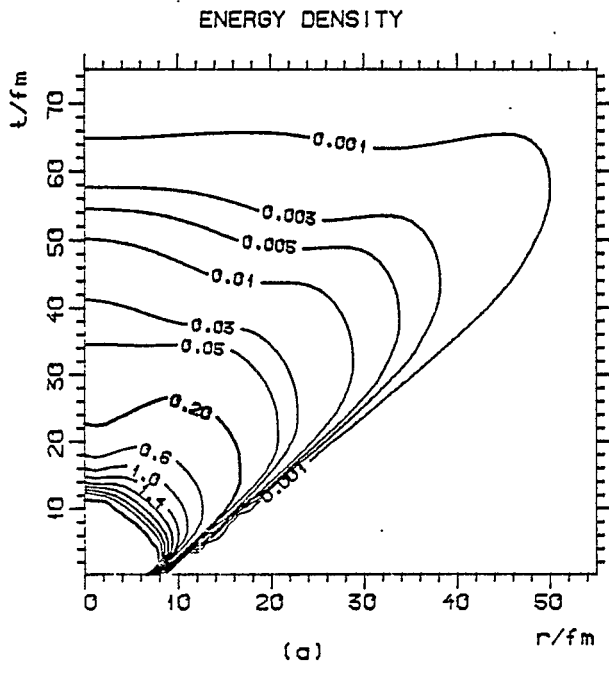


Fig. 2.3

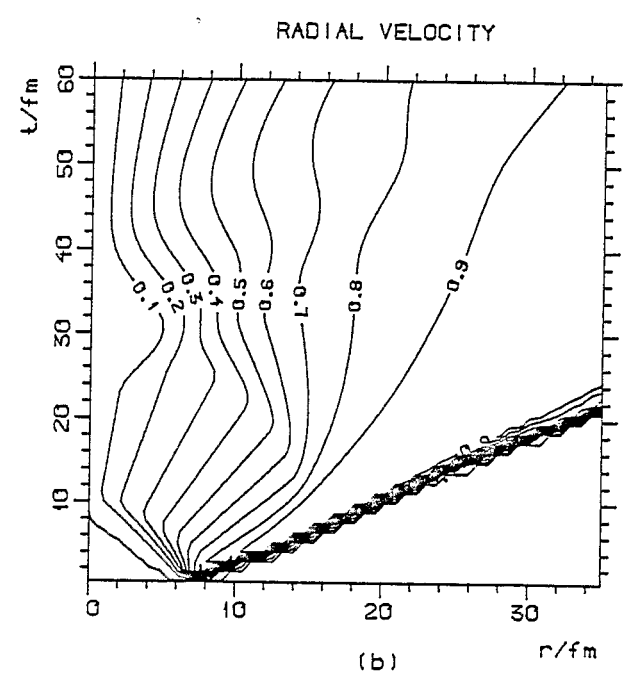
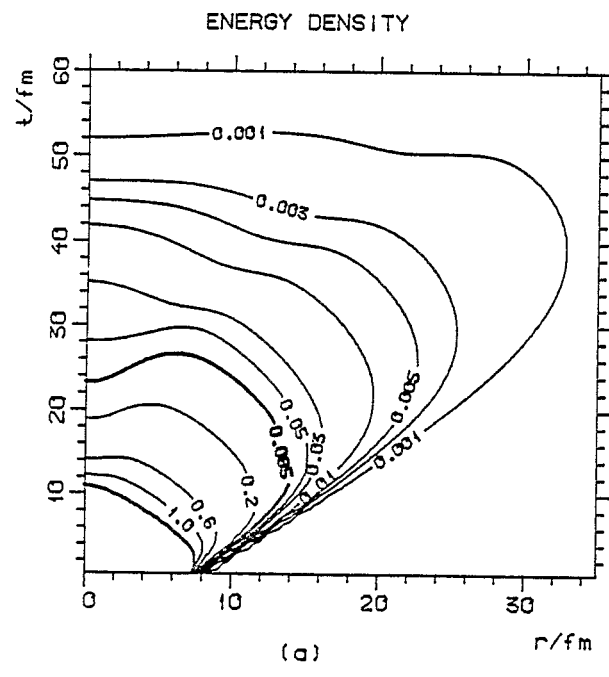


Fig. 2.4

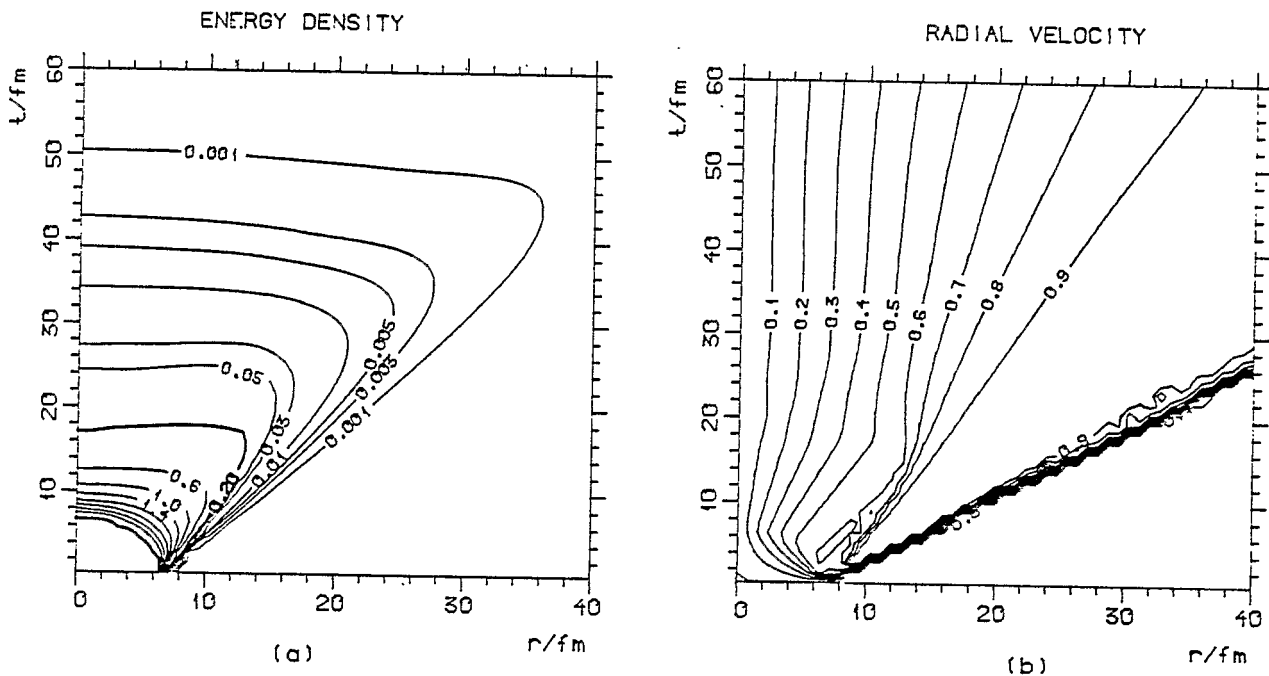


Fig. 2.5

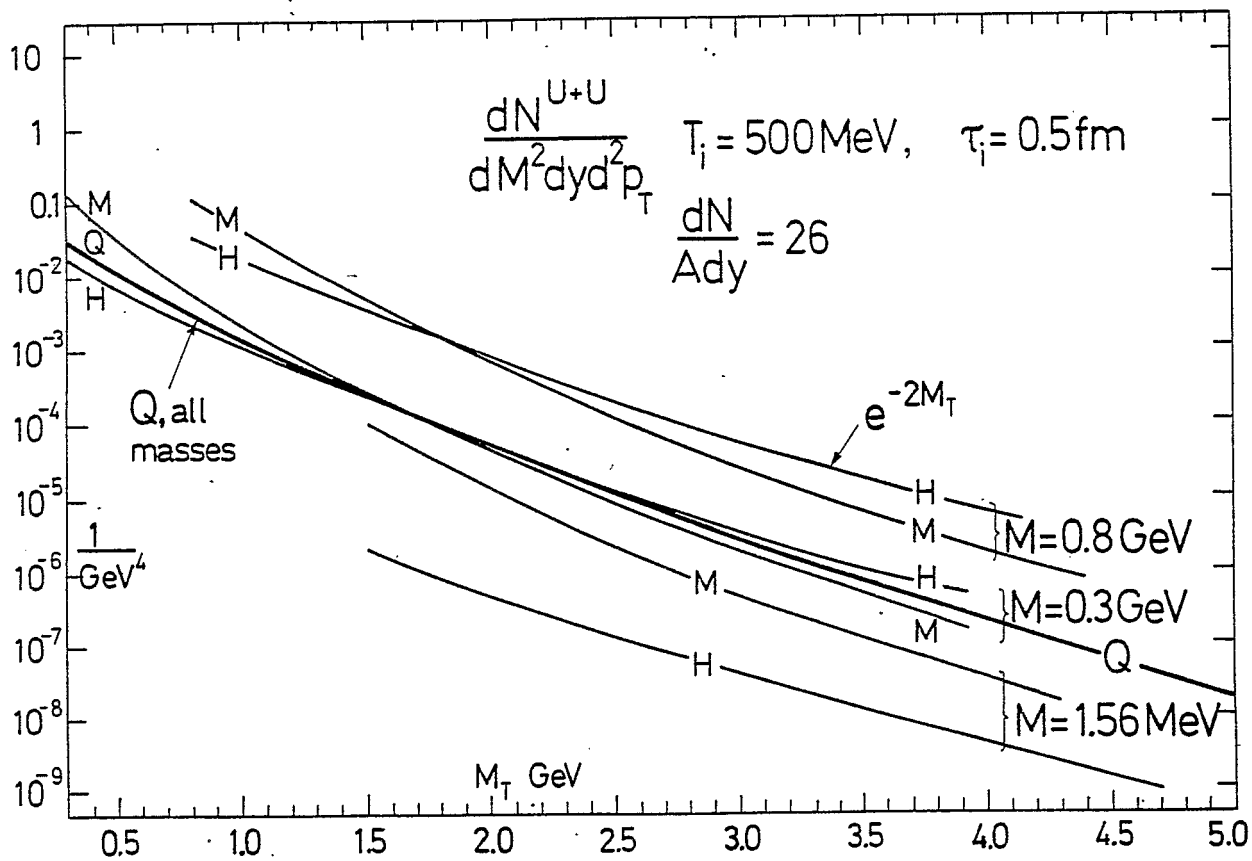


Fig. 4.1

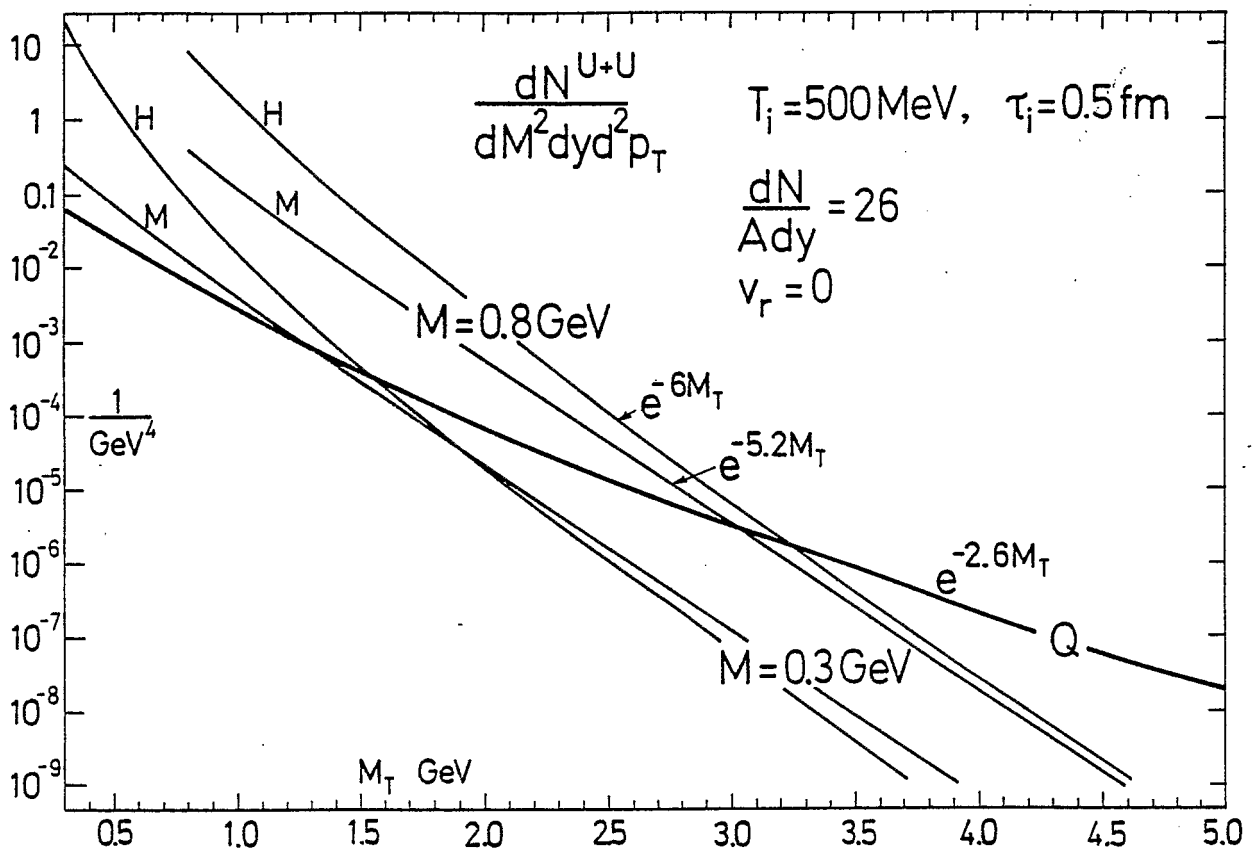


Fig. 4.2

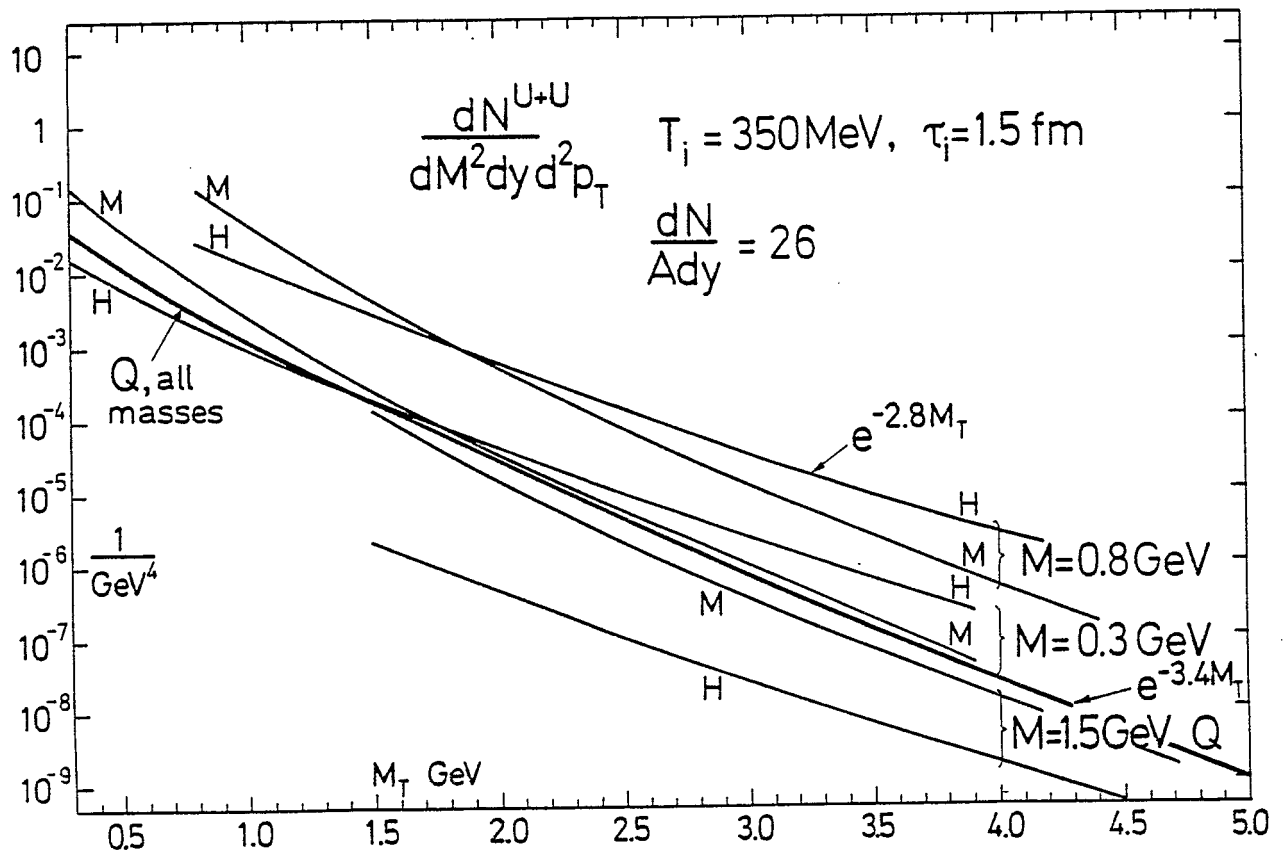


Fig. 4.3

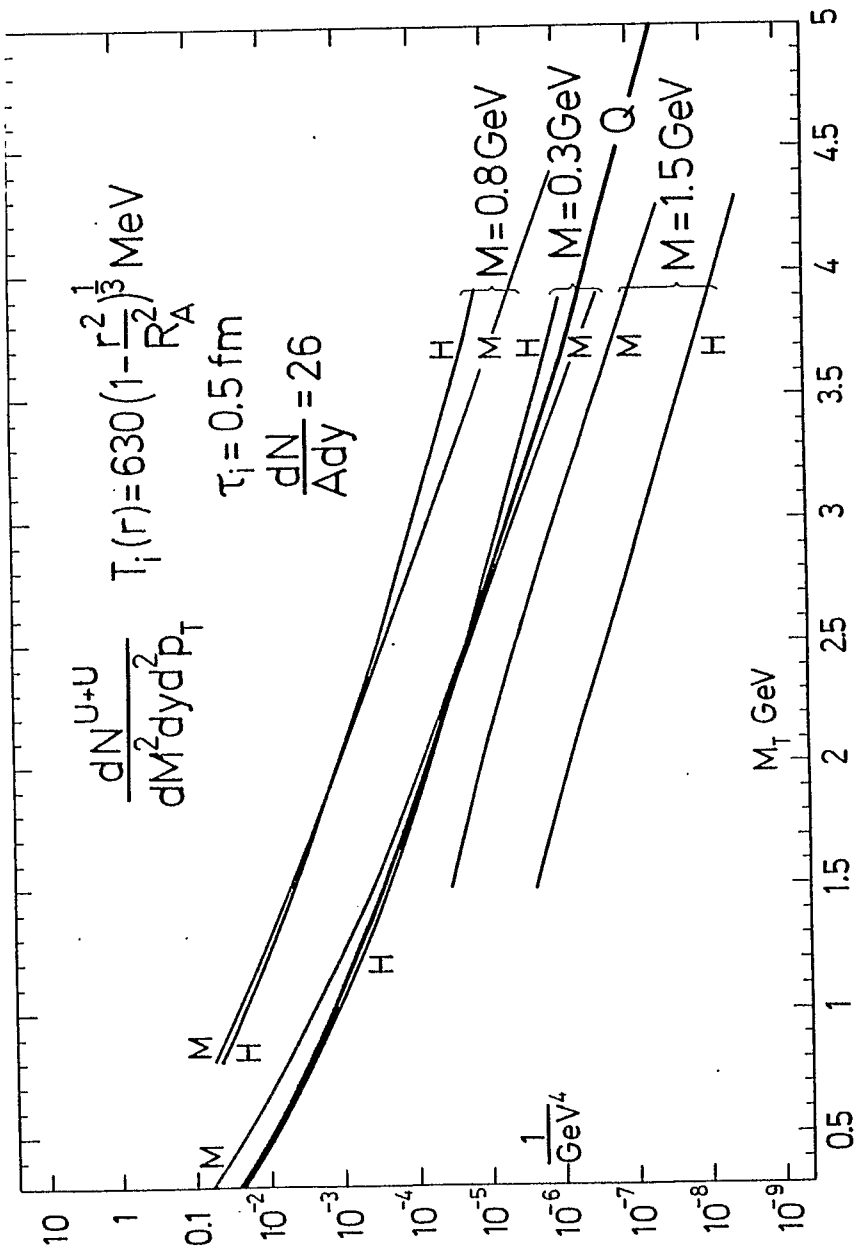


Fig. 4.4

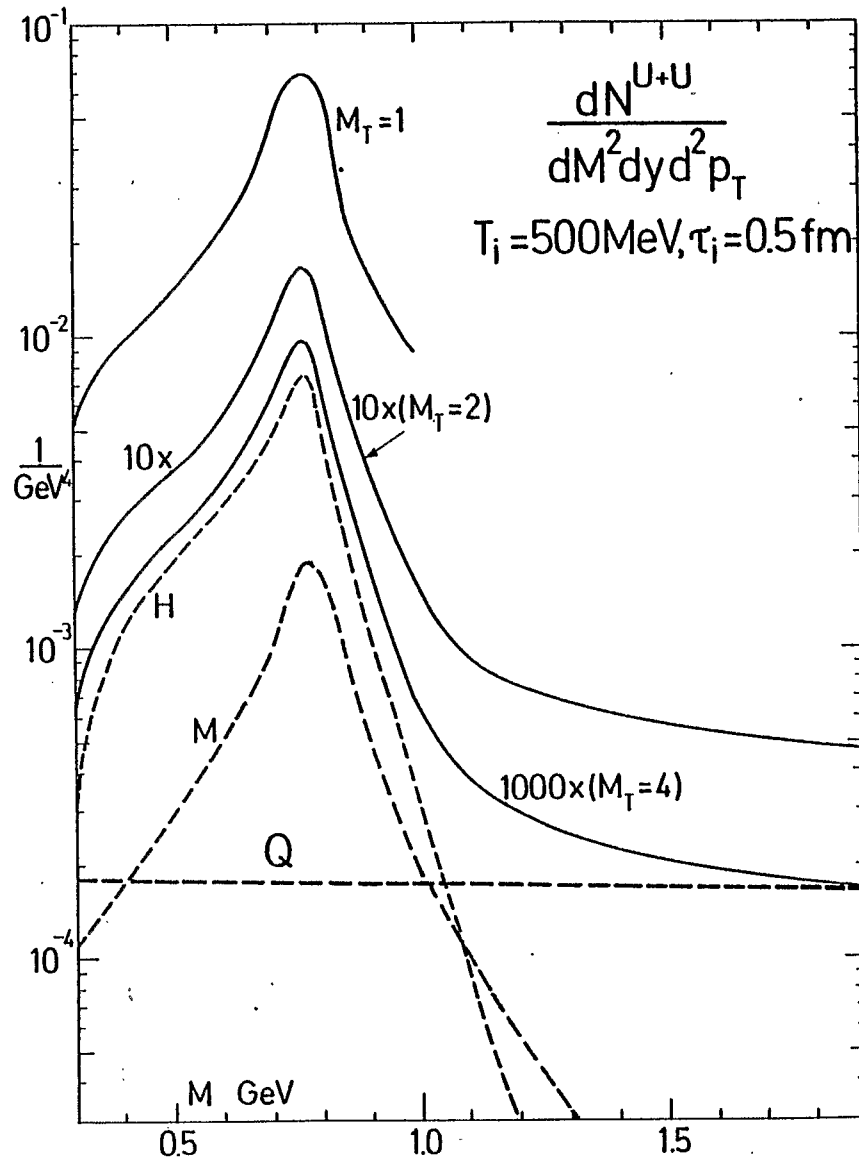


Fig. 4.5

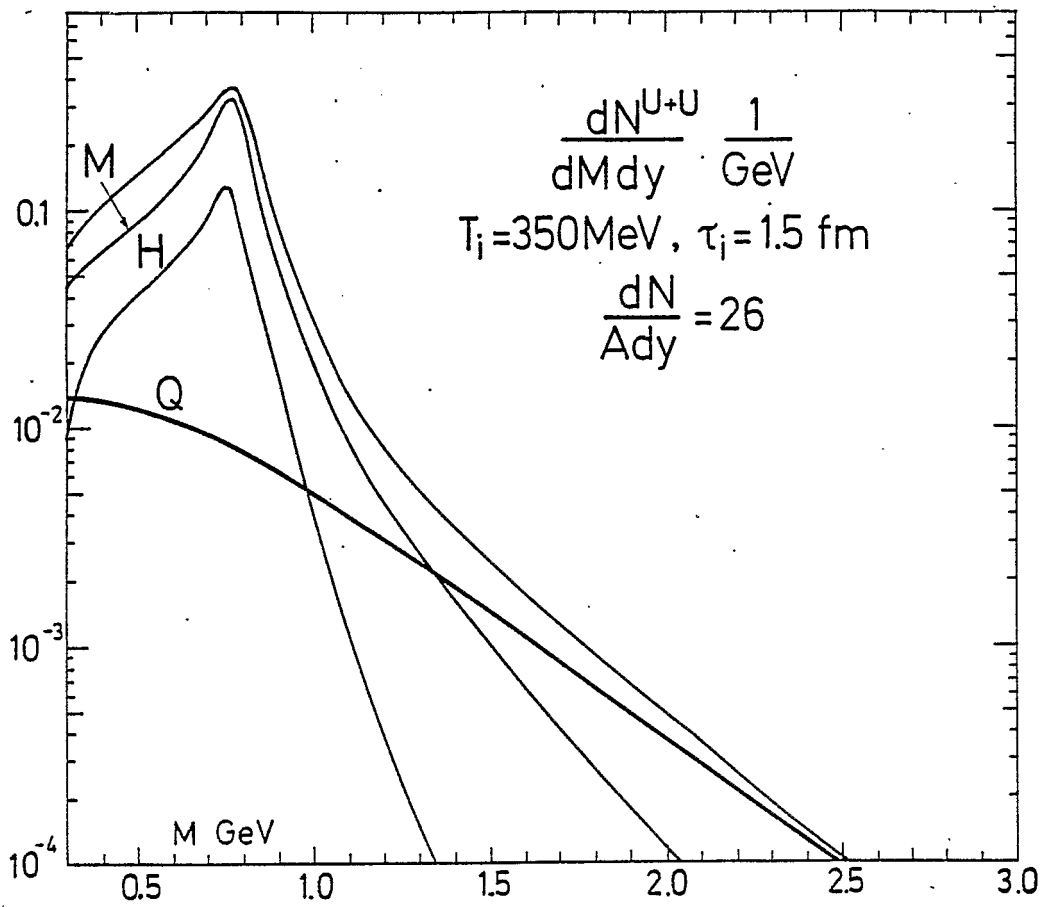


Fig. 4.6(a)

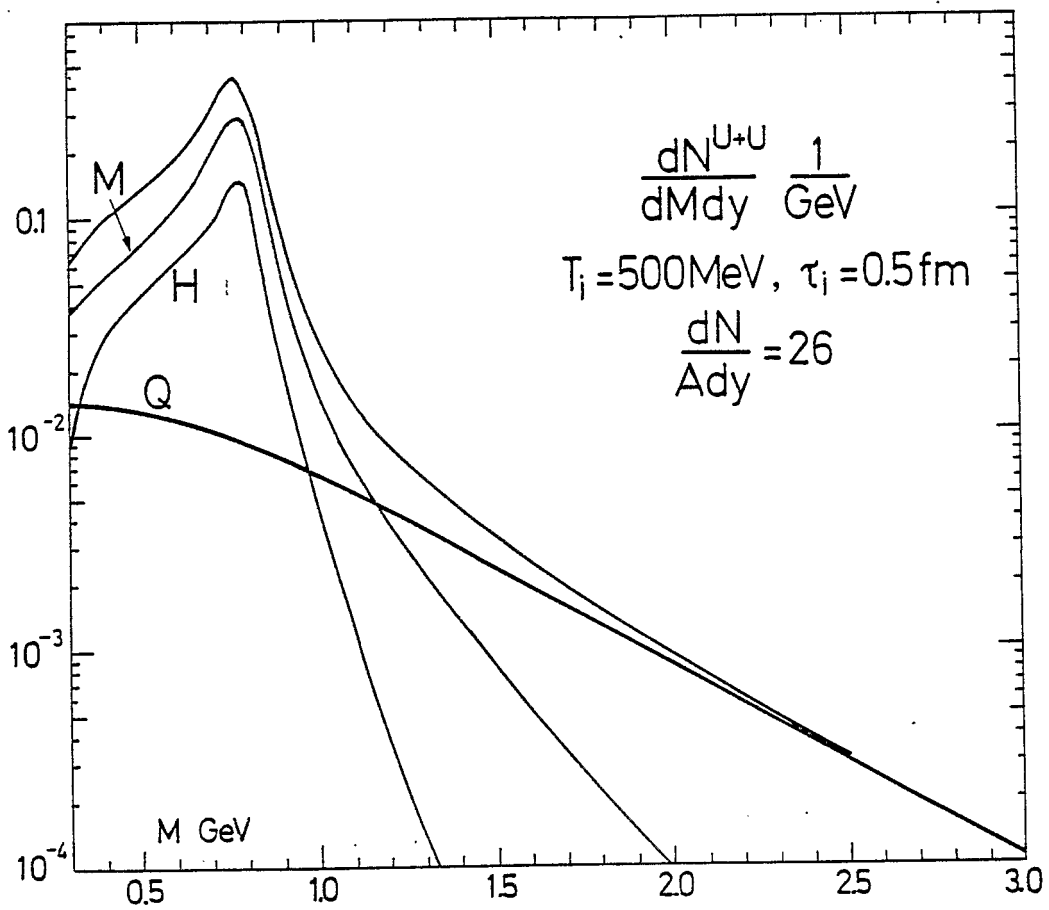


Fig. 4.6(b)

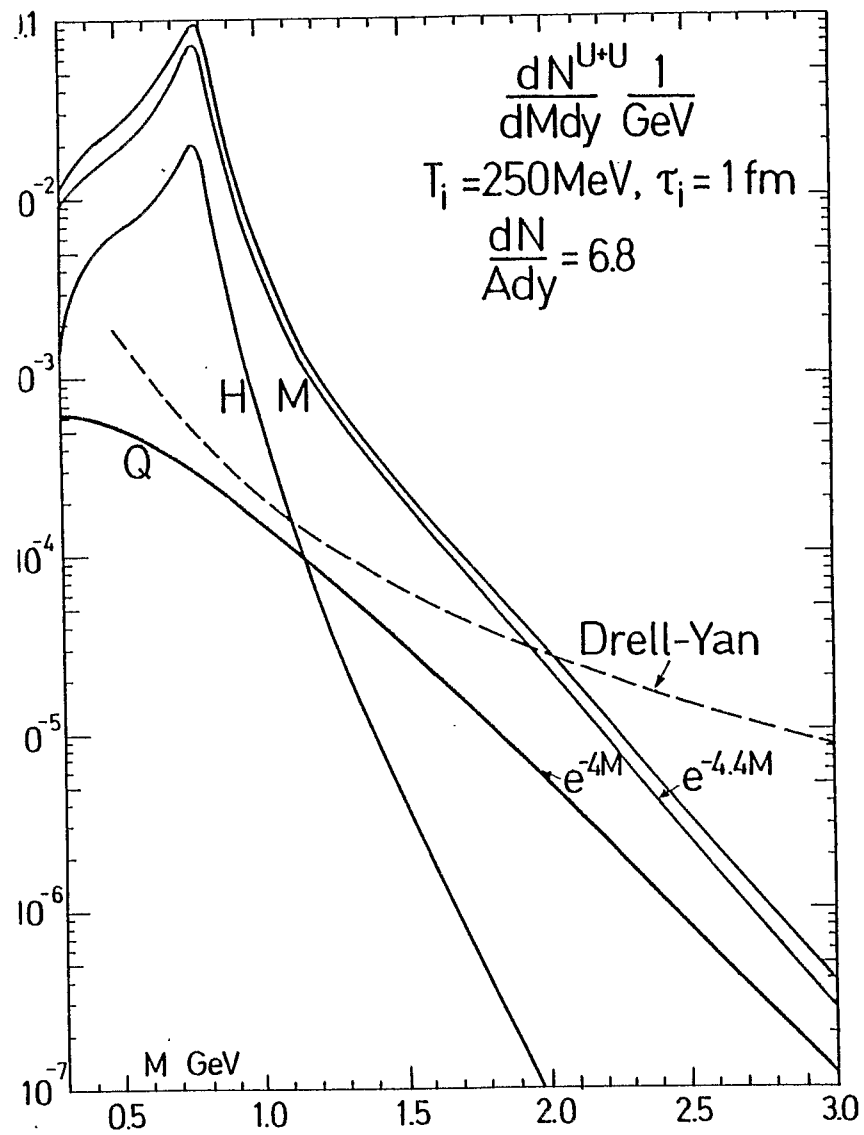


Fig. 4.8